

## High Pressure Properties of $ZnSe_xS_{1-x}$ Single Crystals

SHIRLEY TIONG-PALISOC\*

Physics Department, De La Salle University  
2401 Taft Avenue, Manila, Philippines

The static phase transition points of  $ZnSe$  and  $ZnSe_xS_{1-x}$  ( $0.40 \leq x \leq 1$ ) single crystals in the high pressure region are determined based on the transformation pressures of Bi-III, Bi-III-V and ZnS using the cubic anvil method where the pressure-induced variation of resistance is measured. The transition pressures of the samples vary linearly with the composition of ZnS in the  $ZnSe_xS_{1-x}$ . The shock compression curves of  $ZnSe_{0.40}S_{0.60}$  single crystals are also investigated. The pressure-particle velocity Hugoniot is found to agree with the corresponding Hugoniot of ZnS and ZnSe up to the phase transition point. The P-V isotherm of  $ZnSe_{0.40}S_{0.60}$  derived from the  $U_p$ - $u_p$  Hugoniot is consistent with the calculated P-V curve based on Bridgman's static data of ZnS and ZnSe.

**Key words:** Hugoniot, phase transition, cubic anvil, shock wave, Bridgman, semiconductor

The high pressure polymorph of ZnSe and ZnS, two of the most promising materials for blue light emitting diodes, is of considerable interest. Notwithstanding their wide bandgaps, they undergo semiconductor to metallic phase change characterized by a fall in electrical resistance and a transition to a more closely packed structure. Their pressure-induced phase transition points are among those that made up the fixed-point static calibration curve (Dekker 1966, Le Niendre et al. 1976, Yagi & Akimoto 1976, Ruoff & Chan 1979, Gust 1982). Most of the reported studies are directed toward the measurement of the static transformation pressure. However, there is substantial disagreement in the magnitude of the transformation pressures for ZnSe and ZnS. The experimental results are from different measurement methods and the pressure versus applied load scales are revised several times. Table 1 shows the transition pressures as obtained by various groups. Phase transition studies on the coexistence of two phases were also conducted by Arlt and Ross (1999) by pressure buffering in a diamond anvil cell. The two phases, semiconducting and metallic, of  $ZnSe_xS_{1-x}$  coexist

statically as in a diamond anvil cell. Furthermore, the effects of high pressure on band structure was studied by Allam and Adams (1999) as they investigated the "universal" (i.e. as set upon by the National Bureau of Standards) scaling of impact ionization. High pressures will close the wide bandgaps in ZnSe and ZnS as manifested by a phase transition.

It will be quite noteworthy if the transition points of ZnSe, ZnS and  $ZnSe_xS_{1-x}$  are measured by the same method statically and compared with dynamical results as obtained from shock wave loading. This study aims to report the pressure-induced static phase transformation points of  $ZnSe_xS_{1-x}$  using the resistance variation method and present the Hugoniot curves of  $ZnSe_{0.40}S_{0.60}$  derived by means of shock wave loading.

Table 1. Phase transition pressures in GPa.

ZnSe	ZnS	Author(s)
15.0	18.5	Balchan & Drickamer (1961)
15.0	24.0	Drickamer (1970)
13.7	15.0	Pjermarini & Block (1975)
N/A	15.0	Le Niendre et al. (1976)
N/A	16.2	Yagi & Akimoto (1976)
14.6	17.4	W.H. Gust (1982)

\*Corresponding author: cosstp@dlu.edu.ph

### Static Calibration Curve

Semiconductor to metal transitions are ideal calibration markers on a fixed point pressure scale because associated with the transition is a decrease in electrical resistance of several orders of magnitude that can be easily detected and measured (Block et al. 1977). They provide convenient calibration points for high pressure apparatus where the electrical resistance variation measurement is utilized.

Sintered MgO is used as transmitting medium instead of the conventional pyrophyllite since the latter may cause a reduction of the pressure value at high temperatures. Moreover, gaskets are used to produce a hydrostatic environment for the sample. In ungasketed samples, the region of maximum pressure originates in the central area and decreases radially at the edge of the anvil. There is usually a large pressure distribution across the sample in the ungasketed method. In experiments conducted under nonhydrostatic conditions, the presence of stress gradients and the unknown magnitude of stress often cast serious doubt on the interpretation of the desired measurements. In the gasketed method, these undesirable effects are eliminated. The usage of gaskets also offers the advantage of prolonging the useful lifetimes of the anvils and of allowing maximum pressure to be obtained without anvil failure.

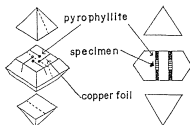


Figure 1. Cross section of the octahedral MgO pressure-transmitting medium.

### Methods, Results and Discussion

ZnSe and ZnS are known to undergo semiconductor to metallic phase change. Their pressure induced phase transition points are among those that made up the fixed-point static calibration curve (Balchan & Drickamer 1961, Drickamer 1970, Piermarini & Block 1975, Le Niendret et al. 1976, Ruoff & Chan 1979). Utilizing the transition pressure of ZnS as obtained by Piermarini and Block (1975) and those of Bi I-II and Bi III-V (as agreed upon in the 1968 International Conference of the National Bureau of Standards), the phase transition points of  $ZnSe_xS_{1-x}$  ( $0.40 \leq x \leq 1$ ) are determined wherein the pressure-induced variation of electrical resistance is measured.

In this study, very high pressures are generated within the 6-8 split sphere vessel with a pressure-transmitting medium which are finally compressed in a 5,000-ton uniaxial press and electrical measurements are subsequently conducted. The samples used are  $ZnSe_xS_{1-x}$  single crystals grown by the self-closed sublimation method with a necked ampule. Figure 1 shows a cross section of the octahedral MgO pressure-transmitting medium, which is 14 mm to a side. Two to four holes (0.8-mm diameter) are drilled through the medium wherein each were

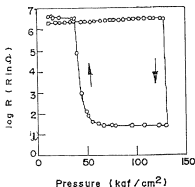


Figure 2. Behavior of resistance with respect to pressure.

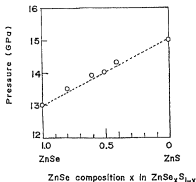


Figure 3. Relationship between static transformation pressure and the ZnSe composition in  $ZnSe_xS_{1-x}$ .

inserted with crushed crystallites of the samples and 3.0 - 3.1 mm-long, Cu strip-covered pyrophyllite bars acting as electrodes are thrust in from both ends of each hole. The pressure-transmitting medium is then held by a tungsten carbide cube made of 8 separate anvils insulated from each other by cardboard and fluorine-enriched resined adhesive tape and gaskets made of pyrophyllite are utilized.

The variation of the electrical resistance is observed in the loading stage for most of the samples. From 3 - 4 M $\Omega$ , the corresponding resistances of ZnSe, ZnSe $_{0.85}$ S $_{0.15}$ , and ZnS dropped abruptly to about a 100 $\Omega$  for ZnSe and ZnSe $_{0.85}$ S $_{0.15}$ , and 2 - 3 k $\Omega$  for ZnS. Figure 2 shows the behavior of the resistance of ZnSe $_{0.85}$ S $_{0.20}$  with respect to pressure using a 10-mm octahedral MgO pressure-transmitting medium. In the loading stage, the resistance has a very sluggish increase from 1.95 M $\Omega$  to 2.55 M $\Omega$  and falls rapidly when the applied oil pressure is 131 kgf/cm $^2$ ; after which, the resistance drop is observed for 10 min. With the pressure released, the resistance does not immediately return to its original value. It is only after one-third of the pressure has been deloaded that resistance starts to increase. After another one-third of the pressure has been released, the resistance returns to its former value at a fast rate.

The semiconductor to metallic transition pressure of ZnSe is determined to be  $13.0 \pm 0.4$  GPa using as calibration points the static transformation pressures of Bi II-III, Bi II-V, and ZnS which are  $2.550 \pm 0.006$  GPa,  $7.7 \pm 0.3$  GPa, and  $15.0 \pm 0.5$  GPa, respectively. Employing the transition pressure of ZnSe obtained in this work as fixed point together with the aforementioned calibration points, the phase-transition pressures of ZnSe $_{0.85}$ S $_{0.20}$ , ZnSe $_{0.85}$ S $_{0.25}$ , ZnSe $_{0.50}$ S $_{0.50}$ , and ZnSe $_{0.40}$ S $_{0.60}$  in units of GPa are determined as interpreted from experimental results where oil pressure is measured in kgf/cm $^2$ . Figure 3 shows the pressure-induced phase transition points of ZnSe $_{0.85}$ S $_{0.20}$ , ZnSe $_{0.85}$ S $_{0.25}$ , ZnSe $_{0.50}$ S $_{0.50}$ , ZnSe $_{0.40}$ S $_{0.60}$ , and ZnS, respectively. The transition pressure has an almost linear variation with increasing ZnS composition in ZnSe $_{0.85}$ S $_{0.15}$ .

#### HUGONIOT CURVES OF ZnSe $_{0.85}$ S $_{0.15}$

Aside from the measurement of the static transformation pressure, the Hugoniot curves (shock velocity - particle velocity,  $U_s - U_p$  and pressure - particle velocity,  $P - U_p$ ) of ZnSe $_{0.85}$ S $_{0.15}$  single crystals are determined and the aforementioned curves are compared with those obtained by Gust (1982) and Bridgman (1948).

To obtain the shock compression curve, a single-stage powder gun is used. The sample assembly is shown in Fig. 4. It employed the pin-contactor method

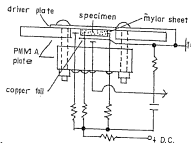


Figure 4. Schematic diagram of a sample assembly for shock wave loading.

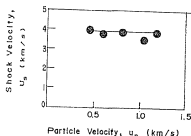


Figure 5. Shock velocity vs. particle velocity of ZnSe $_{0.85}$ S $_{0.15}$ .

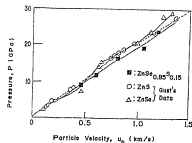


Figure 6. Pressure vs. particle velocity relationship of ZnSe $_{0.85}$ S $_{0.15}$ , ZnS and ZnSe.

(Duvall & Fowles 1963) to measure the shock wave velocity through the specimen. A test specimen with the size of approximately  $5 \times 5 \times 2$  mm $^3$  is fixed on the rear surface of a 1.0-mm thick copper driver plate. Three tilt pins each of which is equipped with a spring are pressed on 12 mm-thick mylar sheets forming the vertices of a triangle with the specimen at the center. The tilt pins function to determine the inclination or tilt

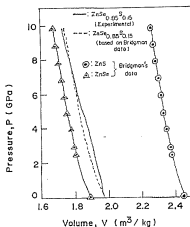


Figure 7. Pressure vs. volume relationship of  $ZnSe_{0.95}S_{0.05}$ , ZnS and ZnSe.

of the shock wavefront in the sample. The end pin which detects the shock wavefront that is propagated through the specimen is pressed on a 12  $\mu\text{m}$ -thick mylar strip and a 15  $\mu\text{m}$ -thick copper strip on top of the center of the rear surface of the specimen. The electric signals from the pins which carry the information of the time required for the propagation of the shock wavefront through the sample and the inclination of the shock wavefront are monitored from the outgoing circuits. The sample is struck by a 2.5 mm-thick copper flyer plate accelerated by a single-stage powder gun whereby the impact velocity is measured by the magnet flyer method (Kondo et al. 1977).

The  $U_1 - U_0$  Hugoniot of the specimen is shown in Fig. 5. In this case, the  $U_0$ 's are determined by the impedance match method using experimental data on the shock wave velocity and the flyer impact velocity. Normally, the impedance method used in this data analysis produces errors in up if a compressed material undergoes plastic deformation or phase transition. Nevertheless, the deviation from linear relationship may be attributed to the differences among the samples used. The uniform shock wave velocity can be explained by the fact that only the elastic wave velocity can be measured if it is faster than those of the plastic and/or phase transition waves.

The density,  $\rho$  and the pressure,  $P$  in the shock-compressed state can be determined by employing the basic equations of shock wave which are derived

from mass and momentum conservation laws considering that  $U_1$  and  $U_0$  are previously known. The initial density of the test specimen is measured to be 5.07  $\text{g/cm}^3$ .

The  $P - U_0$  Hugoniot translated from the  $U_1 - U_0$  Hugoniot is shown in Fig. 6. Comparing the experimental results with Gust's data (1982), it can be inferred that the sample may have undergone a phase change. Although the pin-contractor method used in this work can only measure the elastic wave, the data extrapolated agree very well with the corresponding  $P - U_0$  Hugoniot of ZnS and ZnSe up to the phase transition point in the first plastic wave region notwithstanding the fact that the impedance match method used may have produced errors if the sample under consideration have undergone plastic deformation or phase transition. Figure 6 indicates that the errors are very minimal since the experimental curve resolved from the  $U_1 - U_0$  Hugoniot to a  $P - V$  volume curve (Fig. 7) agrees very well with Bridgman's data. It is however unresolved to take the extrapolated data on the second plastic wave region since this can involve substantial errors.

In order to compare the  $P - V$  Hugoniot measured experimentally in this study with those obtained from Bridgman's static pressure data, the isothermal pressure  $P$  for the test specimen is calculated using the following equation which is derived from Gruneisen's equation of state (Gruneisen 1926).

$$P - P_H = \rho \gamma C_v (T - T_H) \quad (1)$$

where  $P$  is the isothermal pressure,  $P_H$  is the pressure on the Hugoniot,  $r$  is the specimen's density,  $g$  is the Gruneisen parameter,  $C_v$  is the specific heat at constant volume,  $T$  is the room temperature and  $T_H$  is the temperature on the Hugoniot.  $T_H$  is calculated using the thermodynamic equations (McQueen et al. 1970), viz.:

$$\frac{dT_H}{T_H} = -\gamma \frac{dV}{V} + \frac{dS}{C_v} \quad (2)$$

$$2T_H dS = (V_0 - V) dP + (P - P_0) dV \quad (3)$$

In Eq. (3)  $dS$  is solved and substituted in Eq. (2) to obtain the temperature along the Hugoniot. In this work, the product of the Gruneisen parameter,  $\gamma$ , and the density,  $\rho$ , is calculated to be 4.07  $\text{g/cm}^3$  using Soma's (Soma 1980) data for ZnS and ZnSe. The specific heat at constant volume (Soma 1980, Munson and Schuler 1971) is calculated to be

$$C_v = (3739 + 3.80 \times 10^{-3} T - 8.76 \times 10^{-6} T^2) \times 10^6 \text{ (erg/gK)} \quad (4)$$

Figure 7 describes the  $P - V$  Hugoniot of ZnS

and ZnSe calculated from Bridgman's data. Also shown are the experimental data on ZnSe<sub>0.85</sub>S<sub>0.15</sub> which are found to show good fitting to those of ZnSe<sub>0.80</sub>S<sub>0.20</sub> based on Bridgman's data using Munson and Schuler's (Munson and Schuler 1971) formulation, thus verifying further the validity of the measured data.

Up to the phase transition point, the data obtained in this work are valid since the experimental curve resolved from the  $U_s - U_p$  Hugoniot to a  $P - V$  curve fits very well with that based on Bridgman's (Bridgman, 1948) data. Before the phase transition pressure, the  $P - V$  Hugoniot of ZnSe<sub>0.80</sub>S<sub>0.20</sub> agree very well with those corresponding to ZnS and ZnSe.

## Summary

The mechanical properties of ZnSe<sub>1-x</sub>S<sub>x</sub> (0.40 ≤ x ≤ 1) are evaluated. The high pressure polymorph of these crystals are analyzed by measuring their respective semiconductor to metal transition points using the electrical variation method. Electrical measurements are conducted and the resistance drops from 3-4 MΩ to about a hundred Ω for ZnSe and ZnSe<sub>0.80</sub>S<sub>0.20</sub> and 2-3 kΩ for ZnS. Based on the transition point of ZnSe, the transition points of ZnSe<sub>0.80</sub>S<sub>0.20</sub>, ZnSe<sub>0.65</sub>S<sub>0.35</sub>, ZnSe<sub>0.50</sub>S<sub>0.50</sub> and ZnSe<sub>0.40</sub>S<sub>0.60</sub> are experimentally determined and are hereby reported to have a linear variation with increasing ZnS composition in ZnSe<sub>1-x</sub>S<sub>x</sub>. The Hugoniot curves of ZnSe<sub>0.85</sub>S<sub>0.15</sub> single crystals are also determined and compared with the results of Gust (1982) and Bridgman (1948). The pressure-particle velocity Hugoniot implies that the crystal has undergone a phase change and the extrapolated data agree very well with those of ZnSe and ZnS as reported by Gust. The  $P - V$  curve resolved from the experimental  $U_s - U_p$  Hugoniot also agrees very well with Bridgman's data (Bridgman, 1948). It is concluded then that at very high pressures, ZnSe<sub>1-x</sub>S<sub>x</sub> undergoes a phase change from semiconductor to metallic state.

## Acknowledgment

The author wishes to thank the Institute for the Study of the Earth's Interior and the Faculty of Education of Okayama University where the experiments were conducted. She also expresses her gratitude to Prof. E. Ito, Prof. K. Kani, and Prof. M. Hiramatsu for invaluable discussions and to Mr. Yasushi Matsushima for technical assistance. This

work was supported in part by a Grant-in Aid for Scientific Research from the Ministry of Education, Science and Culture, Japan.

## References

- Art T & Ross A. 1999. Pressure buffering in a diamond anvil cell. *Mineralogical Magazine* 20: 12-13.
- Allam J & Adams AR. 1999. High pressure measurements and the "universal" scaling of impact ionization with bandstructure. *Phys. Stat. Sol. (b)* 211:335-344.
- Balchan A & Drickamer H. 1961. High pressure electrical resistance cell, and calibration points above 100 kilobar. *Rev. Sci. Instrum.* 32: 308-313.
- Block S, Forman R & Piermarini G. 1977. Pressure and electrical resistance measurements in the diamond cell. In: *High Pressure Research* (eds. Manghni MH & Akimoto S). Academic Press, New York, p.502-508.
- Bridgman P. 1948. The compression of 39 substances to 100,000 KG/CM<sup>2</sup>. *Proc. Am. Acad. Arts and Sci.* 76: 55-69.
- Decker D. 1966. Equation of State of Sodium Chloride. *J. Appl. Phys.* 37: 5012-5014.
- Drickamer H. 1970. Revised Calibration for High Pressure Electrical Resistance Cell. *Rev. Sci. Instrum.* 41:1667-1668.
- DuVall G & Fowles G. 1963. In: *High Pressure Physics and Chemistry*. Vol.2. Academic Press, London. p. 209.
- Gruneisen E. 1926. *Handbuch der Physik* Vol. 10. Verlag J. Springer, Berlin. p.22.
- Gust W. 1982. Shock induced transition stresses for zinc sulfide and zinc selenide. *J. Appl. Phys.* 53: 4843-4846.
- Kawai N. 1966. In: *A Static High Pressure Apparatus With Tapering Multipiston Formed A Sphere I*. *Proc. Japan Acad.* 42: 358 - 388.
- Kondo K, Sawaoka A & Saito S. 1977. Magnetoflyer method for measuring gas-gun projectile. *Rev. Sci. Instrum.* 48: 1581-1582.
- Le Niendre B, Suite K & Kawai N. 1976. High temperature and high pressures 8:1.
- McQueen R, Marsh S, Taylor J, Fritz N, & Carter W. 1970. *High Velocity Impact Phenomena*. Academic Press, New York. pp.294-299.

- Munson D & Schuler K. 1971. Hugoniot Predictions for mechanical mixtures. In: Proc. 17<sup>th</sup> Segamore Army Mat. Res. Conf., New York. Syracuse Univ. Press, New York. 1070 p. 185.
- Piermarini G & Block S. 1975. Ultrahigh pressure diamond-anvil cell and several semiconductor phase transition pressures in relation to the fixed point pressure scale. *Rev. Sci Instrum.* 46: 973-979.
- Ruoff A & Chan K. 1979. In: High Pressure Science and Technology Vol.1 (eds. K.D. Timmerhaus and M.S. Barber). Plenum, New York. p.779.
- Soma T. 1980. Thermal expansion and lattice dynamics under pressure. *Solid State Com.* 34:927-932.
- Yagi & Akimoto. 1976. Pressure fixed points between 100 and 200 kbar based on the compression of NaCl. *J. Appl. Phys.* 47: 3350-3354.